# Photovoltaic Degradation Analysis and Simulated Models

Shay Mathews[1], Timothy Peshek[2], Yang Hu[2], Roger H. French[2]

Case Western Reserve University

[1]Department of Physics and Engineering
[2]Department of Materials Science and Engineering

May 2, 2014

# Table of Contents

# 1 Introduction

## 1.1 Background

As the cost of PV technology has decreased, making the technology more and more attractive as a large-scale power producer, reliability is playing a greater role in the return-on-investment considerations. The focus of this one year long project was PV lifetime & degradation science (L&DS) and simulated models. L&DS focuses on how and why materials degrade and how long they will last in the real world. Simulated models imitate the electrical behavior of PV panels and are able to give insight into the physical phenomena occurring within a panel. By studying the physical mechanisms by which PV cells degrade, design modifications can be implemented to create longer lasting PV panels. As such, this project seeks to show that simulated models can be used for L&DS studies.

### 1.1.1 *Lifetime & Degradation Science*

Degradation is often studied by observation of PV panels' performance and physical-mechanical characteristics (power loss, cracking, moisture ingress, etc…) in real world installations. To characterize power (or efficiency) loss, the maximum power point is recorded at regular times. System stressors (such as temperature, irradiance, and humidity) that may be correlated with power loss are also recorded at regular times. Time series analysis of these data under varying real world conditions reveals information about degradation modes and processes. A correlation between peak power and system stressors may be sought and characterized in time.

Recent improvements have been made in the field of L&DS to create sound statistical relations to predict and analyze lifetime through the development of degradation pathways [1]. These studies trace pathways beginning at system stressors, moving through system responses, and ending with performance loss. System response metrics include visible cracking, yellowing, and moisture ingress. Other such system response metrics have been developed and tested such as photobleaching due to incident light [2]. This shows that L&DS studies are improved by

gaining more metrics for quantizing the systems' performance and degradation. These studies therefore rely on the amount and quality of data available to answer crucial questions about degradation. This project will seek to develop methods making use of the full current vs. voltage (I-V) curve to provide additional metrics and insight into degradation pathways by using the equivalent circuit model. The selection of parameters and parameter extraction techniques was a major objective of this project.

### 1.1.2 *Simulated Models*

The full I-V curve of a solar panel defines its electrical behavior. However, only the maximum power point is tracked in current L&DS studies as a performance metric. When a conclusion is made that the maximum operating point of a panel has decreased in time, nothing can be said about what changes in the I-V curve have brought about this change. A possible loss of information occurs due to the difficulty of assigning quantifiable parameters to the overall shape of the I-V characteristic. Quantization is accomplished via the equivalent circuit simulated model.

The equivalent circuit model uses passive, discrete circuit elements to simulate the electrical behavior of a PV panel. These circuit elements represent fundamental physical information about the operation of the panel [3]. Thus, simulation techniques can be used to track changes in these physical phenomena over time. Once achieved, efficiency losses can be attributed to varying parameters within the model.

## 1.2 Motivation

Extensive research has been published on the PV simulated model. However, this research has not been applied to degradation science nor has appropriate error analysis been performed. These facts have served as primary motivators for this project.

In addition, large quantities of I-V curves were required to perform this study. Going into this project, one year's worth of mostly unused I-V data was already available for analysis from the Solar Durability and Lifetime Extension Center (SDLE) SunFarm on the Case Western campus. This project was partially motivated by the prospect of making use of this I-V data to give insight into degradation and develop methods which with to track and understand parameter values in future degradation studies.

## 1.3 Objectives

The goal of this project was to characterize the degradation processes of PV panels by plotting the parametric changes of the equivalent circuit model over time. This was to be achieved through careful circuit simulations and analysis. The proposed set of objectives entering the project was:

1. Determine the best parameter extraction techniques for big data.
2. Electrically simulate PV panels and apply extraction techniques to simulation data.
3. Understand error due to assumptions, approximations, and noise.
4. Analyze real SunFarm data with the now-understood techniques.
5. Produce plots of parameter values with error bars vs. time.
6. Draw conclusions on degradation from the newly extraction information.

The first four objectives were meant to span most of the year with the last two being executed relatively quickly given that the techniques and algorithms had been developed properly.

# 2 Theory

## 2.1 The Solar Cell

A typical solar cell consists of two distinct regions of differently doped silicon. The top layer is n-type and is connected with the ground of the load while the bottom layer is p-type and is connected with the positive terminal of the load. In Figure 1, the front metal contacts connect the n-type and the back metal contact connects the p-type. In the simplified schematic, these two materials touch in the middle to form a junction in which the electrons from the n-type material combine with the holes in the p-type. As electrons and holes combine, a voltage is built up across the junction and equilibrium is reached, forming a depletion region in between the two layers. The depletion region promotes charge flow in only one direction because of the electric field that builds up [4]. This diode-like behavior is the reason for the cell's ability to generate DC power and will play an important role in the development of the simulated model.

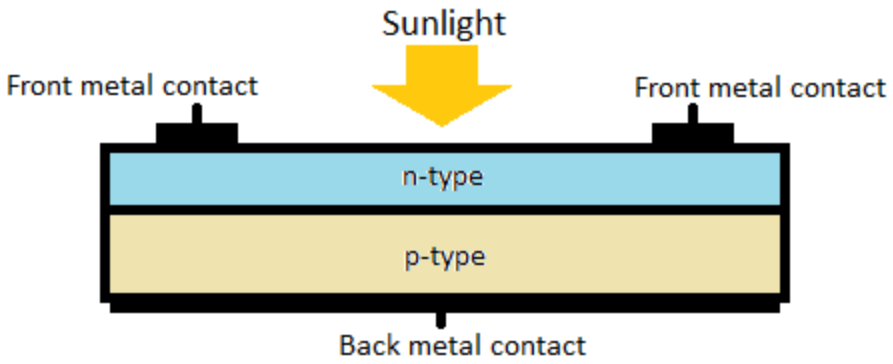


Figure 1: Schematic drawing of a solar cell. The front metal contacts are thin strips of metal meant to let sunlight into the material, and the back metal contact is a sheet covering the entire back.

Incoming photons with energy higher than the band gap energy knock electrons in the n-type material out of their bonds and into the conduction band, making the electrons free to move around the material. As a result, a hole is formed that can be filled with another neighboring electron. The hole, just like the electron, moves around the material. Electron-hole pair generation is proportional to the number and intensities of photons hitting the panel and

results in a current source-like behavior. Generation of electron-hole pairs in addition to the diode-like qualities of the depletion region makes for the generation of power.

An I-V curve is obtained from a solar panel by varying a resistive load from zero to infinite resistance (Infinite resistance simply refers to an open circuit). As the load varies, the current and voltage across it are recorded and plotted, generating a characteristic as shown in Figure 2a. A power vs. voltage relationship may be generated by calculating and plotting IxV vs. V. As shown in Figure 2b, one can load the panel to a certain voltage in order to obtain maximum power output. The y-value of this maximum power point is used as a performance metric in current L&DS studies. Clearly, movement of this point results from intricate shifts in the slope of the I-V curve.

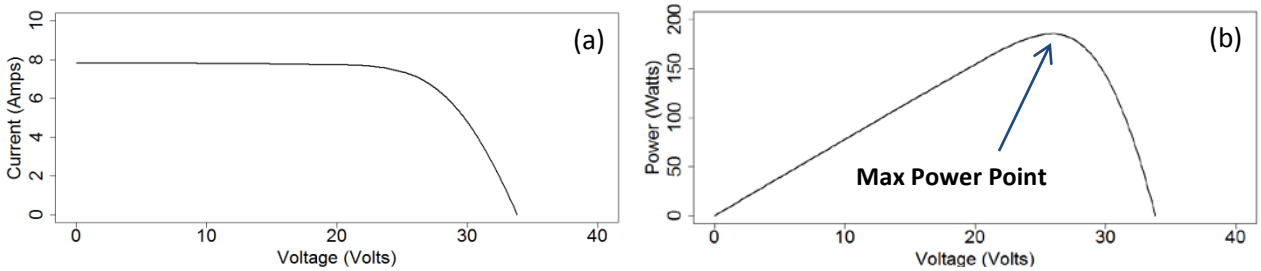


Figure 2: (a) The I-V curve of a typical PV panel. (b) A power vs. voltage (P-V) curve can be obtained from the I-V curve. Maximum power point is shown.

## 2.2 Single Diode Model

### 2.2.1 *The circuit*

It may seem impossible to model the electrical behavior of the PV panel shown in Figure 1 with discrete circuit components. However, by studying the physical phenomena closely, one can conclude that it must involve a current source and diode. These two circuit components are shown on the left side of Figure 3. Together, the current source and diode electrically mimic an ideal solar cell with the bottom of the circuit being the front metal contact (ground) and the top being the back metal contact (positive terminal). The properties of the diode represent the

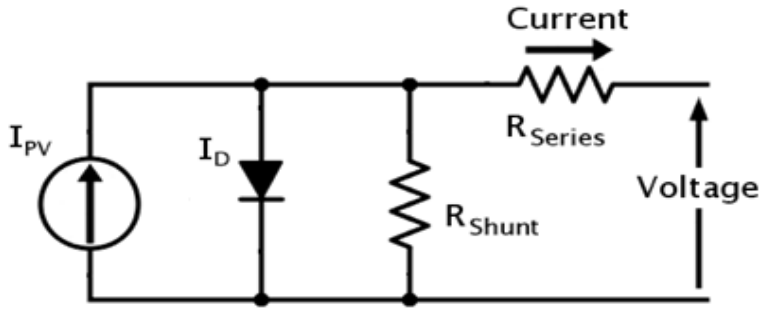


Figure 3: The equivalent circuit model. This circuit will mimic the electrical behavior of a solar cell. The load is attached across the Voltage label on the right hand side.

diode-like behavior of the cell and the current source represents electron-hole generation from incident photons.

The series and shunt resistances account for non-idealities in the solar cell to make the model better fit a real solar cell. By determining the appropriate value of each circuit element, the circuit can closely mimic the electrical behavior of any PV panel. The electrical uniqueness of each panel is accounted for with variations in parameter values.

In order to create an equivalent circuit specific to a selected PV cell, previous studies have developed methods for quantizing characteristics of the physical processes occurring [5], [6]. In order to do so, each circuit element is related to physical phenomena and carefully extracted from the I-V curve.

### 2.2.2 *The equation*

By performing nodal analysis and using the Shockley diode equation on the circuit in Figure 3, the current (I) and voltage (V) can be related as follows:

$$I = I_{PV} - I_0 \left[ \exp\left( \frac{q(V + R_S I)}{n k_B T} \right) - 1 \right] - \frac{V + R_S I}{R_{Sh}} \quad (1)$$

There are 5 major parameters within this model: $I_{PV}$, $I_0$, n, $R_S$, and $R_{Sh}$.

$I_{PV}$ is the photo-generated current, which is dependent on illumination intensity. $R_{Shunt}$ provides the photo-generated current an alternative path in parallel with the load. $R_{Series}$ represents contact resistance between the metal contacts and the pn junction (front and back metal contacts in Figure 1). $I_0$ is reverse saturation current of the diode, n is the ideality factor of the diode, $k_B$ is Boltzmann's constant, T is temperature, and q is the charge of an electron. An important feature of equation (1) is that neither current nor voltage can be isolated on one side of the equation. Therefore, it is impossible to simply fit this equation to an experimental I-V curve and obtain parameter values. While it is possible to extract all 5 parameters from an I-V curve using approximation techniques, this project has focused entirely on series and shunt resistance. The following section describes why.

## 2.3 Selection of Parameters

Within the equivalent circuit model there are two major sources of power loss: series and shunt resistance. These differ in that one is in series with the load while the other is in parallel.

Series resistance acts at high light intensities to account for resistance within the cell and drop the maximum power point voltage. Most electrical power generators have an internal resistance that almost entirely determines their I-V characteristics. Solar cells, however, rely on a pn junction to generate power and their I-V characteristics make this evident. The series resistance exists within the pn junction and acts on the device performance in a secondary manner [7]. Thus, series resistance in the context of this project can be related to the series resistance of a more simple power generator, but must be extracted carefully from the I-V curve. This is because the I-V curve of a solar cell is affected in certain ways by series resistance but is not totally determined by it. Solar cell series resistance is a result of contact resistance on the front and back surfaces of the junction and is a major concern for solar cell manufacturers [8]. The extraction of series resistance will add a system response metric representing these physical phenomena.

Shunt resistance becomes important as light intensity decreases and also has important implications for manufacturers [8], [9]. Sometimes called parallel resistance, the shunt resistor provides current generated by the PV cell an alternate path to flow through in parallel with the load. When multiple cells are connected together (as in a solar panel), often the power generated by each cell varies small amounts. A cell generating more power than its neighbors (called a mismatch) dissipates the extra power through the shunt resistance, causing the cell to heat up [10]. This mismatch has important implications for design and manufacturing of solar cells because a higher shunt resistance will minimize the amount of current flowing in parallel with the load and thus minimize the generation of damaging heat [11]. Shunt resistance arises from scratches and impurities within the cell, which lead to increased recombination [10].

While both series and shunt resistances affect the I-V characteristic secondarily, their approximate values can be extracted and tracked over time. Other parameters in the model are known to be properties of the silicon junction itself and aren't expected to change or account for power efficiency degradation over time [6]. Upwards of 22 different parameter extraction techniques have been developed and extensively tested in literature [12], [13]. This project has largely been concerned with selecting and making use of extraction techniques that are fast and have well-understood errors.

## 2.4 Parameter Extraction Techniques

Previous studies have shown that the extraction of the resistance values must be done carefully, taking into consideration the climate in which the I-V curves were traced [5], [14], [15]. Specifically, "climate" refers to the temperature of the solar panel as well as the irradiance incident on it. Little to no research has been done to understand why this occurs, but have instead focused on its behavior. Regardless, all studies have concluded that extracting parameter values at normal to high irradiance and a relatively narrow range of temperatures sufficiently minimizes the climate error to make its contribution to the total error insignificant [5], [13], [14].

Techniques have been developed that require high computing power based on complex analyses and mathematical functions such as the Lambert W-Function [16]–[18]. Others have made use of iterative techniques that are also computationally complex and are subject to high variability depending on initial user input [19]. The last major class of extraction techniques rely on integration of the I-V curve after spline interpolation of the data [6], [20]. Such smoothing of the data introduces and unknown and variable error that is difficult to approximate. The extraction techniques that are quick and have been verified to be extensively valid for wide ranges of climate conditions and solar panels are presented below.

### 2.4.1 *Shunt Resistance*

Beginning with equation (1), it can be easily deduced that the exponential term is small at low voltages. By approximating it to be zero at low voltage, the following relation is obtained.

$$I \cong \frac{I_{PV} - \frac{V}{R_{Sh}}}{1 + \frac{R_S}{R_{Sh}}} \tag{2}$$

Equation (2) no longer has a transcendental form because the current is isolated on the left-hand side. The second approximation is made through the assumption that, in a normal functioning solar cell, $R_S \ll R_{Sh}$ [5]. With this, equation (2) becomes

$$I \cong I_{PV} - \frac{V}{R_{Sh}}. \tag{3}$$

This straight line equation holds only in low voltage, but reveals a method with which to approximate shunt resistance. A straight best-fit line to the low voltage region of an I-V curve has the slope -1/$R_{Sh}$. A small $R_{Sh}$ makes for a very steep low voltage region in the I-V curve and thus a greatly reduced maximum power point. Previous studies (and my own simulations) show that $\left|\frac{dV}{dI}\right|_{V=0}$ is not dependent on the climate in which the I-V curve was traced [5], [14].

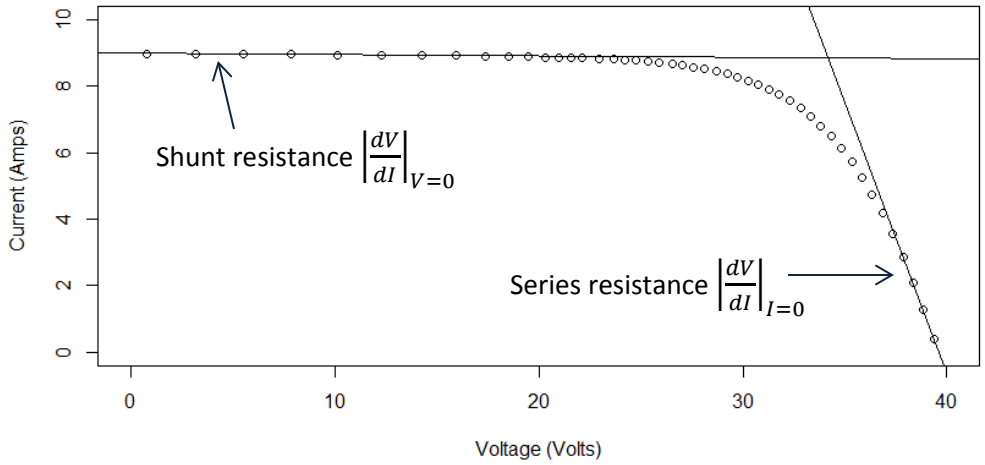


Figure 4: Straight line fits to the two linear regions of the I-V curve are used to determine the values of shunt and series resistance

### 2.4.2 *Series Resistance*

While shunt resistance is related to the slope at low voltage, series resistance is related to the slope in the high voltage region. Khan et al has shown that by manipulating equation (1) and making more assumptions (with negligible error) about the system, the following relation can be obtained [5].

$$\left|\frac{dV}{dI}\right|_{I=0} = R_S + \frac{nk_BT}{q}\frac{1}{\left(I_{SC} - \frac{V_{OC}}{R_{Sh}}\right)} \tag{4}$$

$V_{OC}$ (open-circuit voltage) is the voltage at I = 0 and $I_{SC}$ (short-circuit current) is the current at V = 0. Making use of this equation to determine $R_{Series}$ requires multiple I-V curves recorded at different irradiances at the same temperature. Equation (4) is a straight line equation if $\left|\frac{dV}{dI}\right|_{I=0}$ is plotted as a function of $\left(I_{SC} - \frac{V_{OC}}{R_{Sh}}\right)^{-1}$. The slope of this line is $\frac{nk_BT}{q}$ and the y-intercept is $R_S$. The issue of obtaining multiple I-V curves is not an issue for this project considering the quantity and rate at which data are collected. However, differing irradiances over the course of a day makes for differing temperatures (In fact, irradiance and temperature are highly correlated). This makes for a significant error in the determination of $R_S$ and has been a focus of this project.

A major lack of information in the literature exists concerning the determination of $\frac{dV}{dI}$. I was unable to find any information about how many data points to fit the straight line to. In order to track changes in a parameter over time, a standardized method must be used with an understood error. For example, in the determination of $R_{Sh}$, a fit to the left-most data points is required. Fitting to the left-most 10 points produces different results from fitting the left-most 11. So, this has also been a major focus because my project mainly seeks to provide reliable methods for future L&DS work.

# 3 Simulations

## 3.1 SPICE (Simulated Program with Integrated Circuit Emphasis)

When attempting to extract $R_S$ and $R_{Sh}$ from real data, one does not know the "real" values. This makes error analysis and technique verification difficult. As a solution, I used simulation software to practice extraction techniques and understand error. I was able to build the circuit shown in Figure 3 with arbitrary parameter values and generate I-V curves from it. After obtaining an I-V curve with known parameter values, I applied the extraction techniques and obtained approximate parameter values. This process required an accurate circuit simulator with the ability to generate I-V curves.

SPICE is an industry standard circuit simulator mostly used for complex transient analysis. However, its superb diode modeling and ability to solve complex circuits made it perfect for this project. SPICE has several other qualities that motivated its usage in this project. It allows for custom diode models to be built and used in its simulations. Saturation current ($I_0$) and ideality factor (n) are properties of the diode in Figure 3. SPICE allows a model to be built and used with these values assigned by the user [21]. In addition, SPICE allows quick and easy automated scripts to be written that step through many parameter values. I was able to easily generate an I-V curve with certain parameter values, then increment one of the parameters by a small amount and generate another I-V curve. This allowed for studying the effect of each parameter on the I-V curve individually. Since I planned on applying techniques to thousands of real I-V curves, it was necessary to be able to simulate the same magnitude of data.

## 3.2 Effect of the Parameters

SPICE made it easy to understand the effect that the parameters have on the I-V curve and helped explain the theory more concretely. The below plots show the effects of varying series and shunt resistance on a 60 cell solar panel.

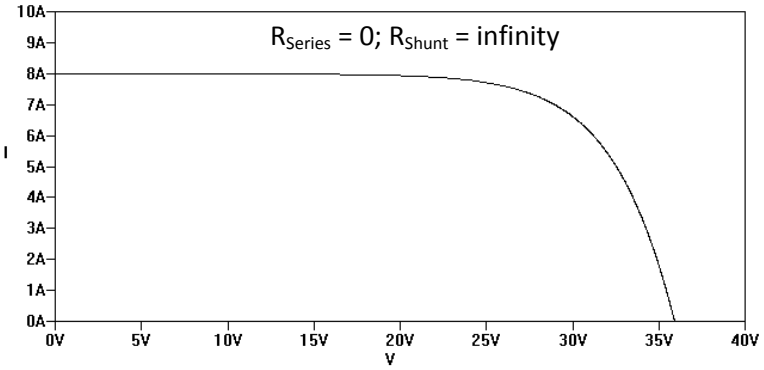


Figure 8: The effects of varying series and shunt resistance. This visually shows why the slope at low voltage is used to determine shunt resistance while the slope at high voltage is used for series resistance. We expect degradation to occur from either increasing series or decreasing shunt resistance.

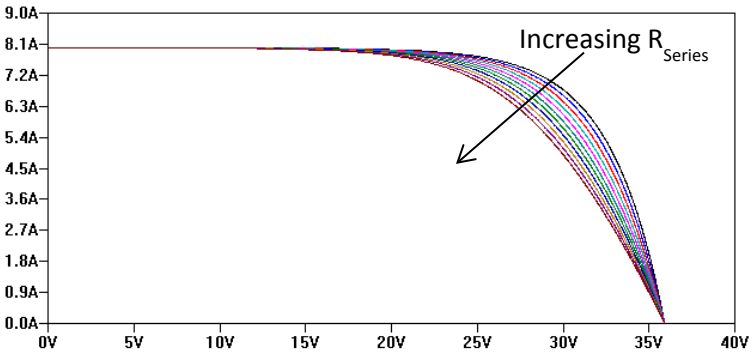


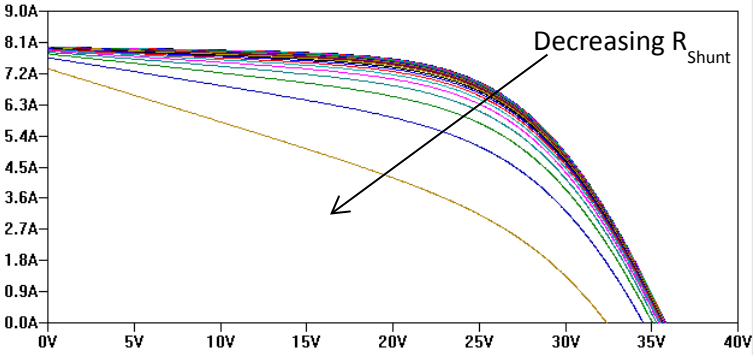


## 3.3 Methods

Since the equations and overall conceptual process for parameter extraction has been developed, I sought to understand the specifics of fitting straight lines to the I-V curve and the dynamics associated with the process.

Assume we have an I-V curve with N ordered pairs of V and I ($V_N = V_{OC}$ and $I_1 = I_{SC}$):

$$(V_1, I_1), (V_2, I_2), \dots, (V_N, I_N)$$

In order to understand how many data points to fit for parameter extraction, I used simulation data and produced plots of percent error vs. number of points fit. Percent error is calculated using the actual value inserted into SPICE and the extracted value from the I-V curve. Number of points fit was converted to a fraction of $V_{OC}$ in order to generalize the results for future use on real data.

SPICE simulations have zero noise, which is very much unlike experimental I-V curves. So, I used the percent error listed on the I-V curve tracer used on the SunFarm to add noise to the simulated I-V curves from SPICE. This made the extraction process realistic and indicative of future work with real data.

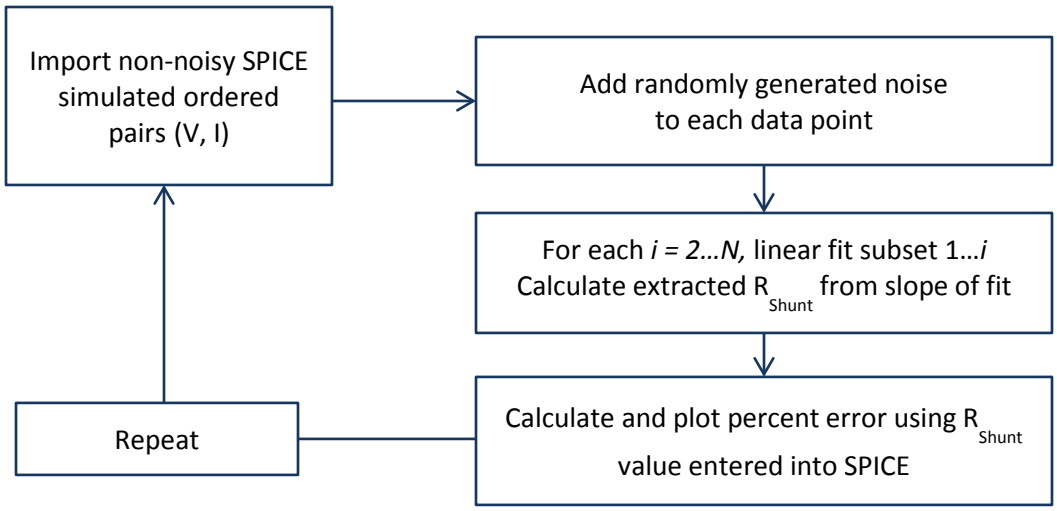


Figure 5: Beginning in the upper left, the process for determining the number of data points to fit for $R_{Shunt}$ determination. I looked for a value of *i* at which percent error was minimized.

## 3.4 Results & Discussion

The process described in Figure 5 proved useful in understanding the best-fit lines and how to use them for I-V curve data. The initial, non-noisy, I-V curve from SPICE is shown in Figure 6. The results from adding noise to it and plotting error in RSh vs. number of points fit is shown in Figure 7.

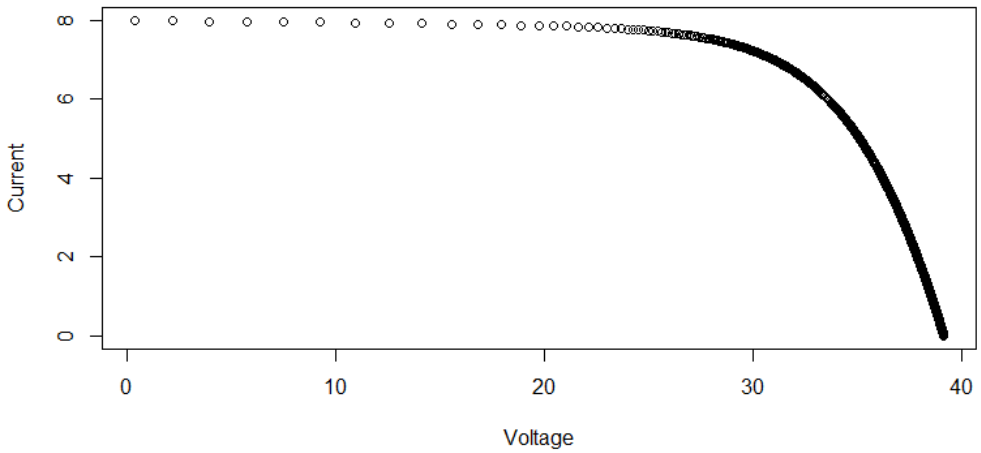


Figure 6: One of the simulated I-V curves used for exploring the best-fit line process

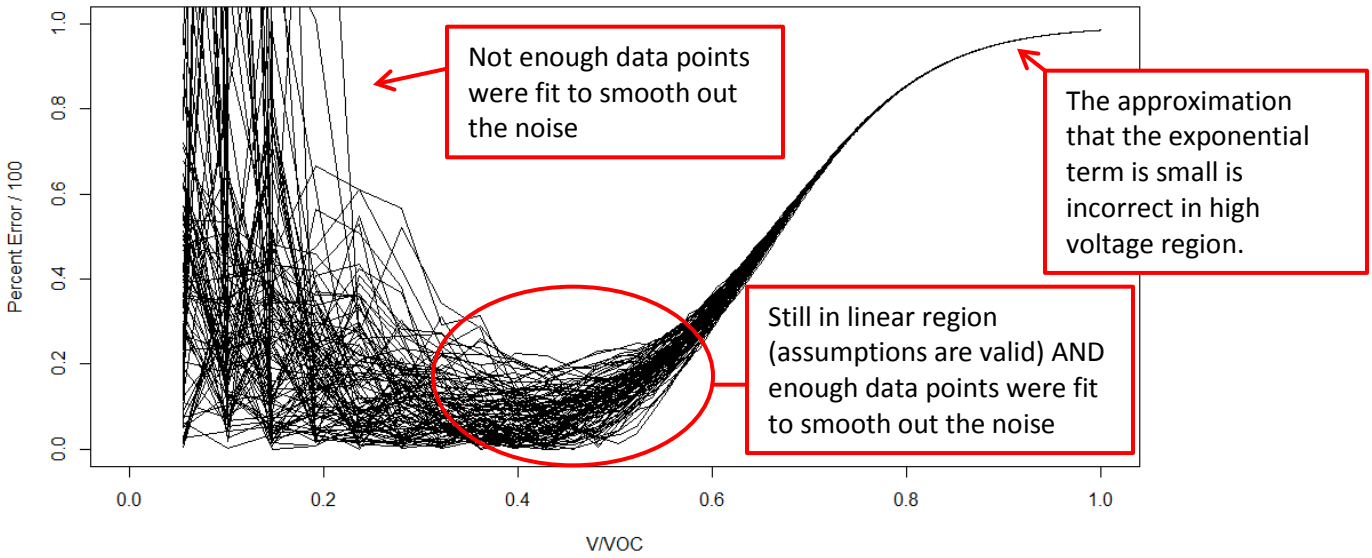


Figure 7: This plot shows that fitting a straight line to all of the data points left of ~0.4$V_{OC}$ minimizes percent error in the extraction of $R_{Shunt}$.

Each line in Figure 7 represents one iteration of the process in Figure 5 with the noise regenerated for each. This accounts for the large variation in fitting a straight line to a small number of data points, shown in the left part of Figure 7. Shown in the right region of the plot, fitting a straight line to the entire I-V curve results in a large error. This is due to the assumption that the value of the exponential term from equation (1) is small in the region that we are fitting. The result is a "sweet-spot" around $0.4V_{OC}$ where neither of these issues exists and the percent error is minimized. I repeated this process for varying parameters and found the same answer each time. These results helped me move forward knowing exactly where to fit the straight line with good understanding of the error associated with it.

# 4 SunFarm Data

The initial goal of this project was to develop parameter extraction techniques and apply them to one year's worth of SunFarm data. This section will discuss the process of acquiring this data and making sense of it. Then, I will show that looking for changes in the parameter values over the course of a year is not worthwhile, because the panels have not shown sufficient degradation at this point in time.

## 4.1 Acquisition and Parsing

The SDLE SunFarm, located in Cleveland, features over 130 PV modules on 14 trackers. Large quantities of data are collected approximately every 10 minutes during day time operation. Weather data includes irradiance, ambient temperature, and wind speed. Module-specific data are collected by the Daystar Multi-Tracer and includes panel temperature and I-V curves. Maximum power point and fill factor are extrapolated from the I-V curves.

Weather data and module-specific data are combined and saved in XML file format. One XML file is created every 10 minutes for each PV module on the SunFarm. Unfortunately, the tree-like XML file format is not friendly to analyzing big data, so it was necessary for it to be converted to a tabular format such as CSV. So, I wrote a Java app that was able to parse large quantities of XML files and output CSV files for analysis. The app allows you to select multiple directories containing up to 5000 XML files per module and choose an output directory. It also allows you to select which attributes to extract from the XML files: weather data, I-V data, or other specific values. I also added the functionality to only get information for a single module instead of having to convert all modules' data. The app first outputs one CSV file per module containing all single value data (everything except I-V curves). Then, one CSV file per I-V curve is exported with an associated time stamp. The app generates code for RStudio to import this data and begin analysis.

## 4.2 R Analytics

All analysis and plotting for this project were done with RStudio, an interactive development environment (IDE) for R programming language. R is an open source, high-level statistical computing language that allows easy analysis and handling of large data sets. The RStudio environment is comparable with that of Matlab, but with a focus on user-created statistics packages. The data structure handling of RStudio makes it perfect for the data science approach to degradation that this project has focused on. The large CSV files exported by my Java app were easily imported into RStudio as data frames, which are able to hold tabular data. To see example R code that I used for generating the fill factor plots in this section, see Appendix A.

## 4.3 Results & Discussion

### 4.3.1 *Single Day*

I first sought to apply the techniques I developed to a single day's worth of data for a single module. Over the course of a day, the parameter values should not be varying. So, this was a way to verify that the techniques were stable enough to detect changes in parameter values.

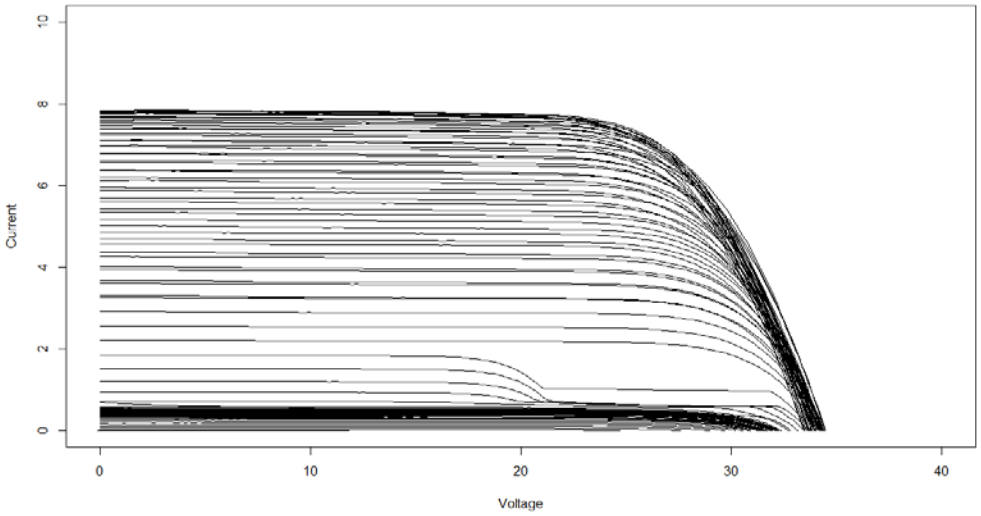


Figure 8: All I-V curves for Canadian Solar 1x module 209 from July 25, 2013.

I chose to analyze the data from July 25, 2013 for a Canadian Solar 1x solar panel. I started by importing the entire days' worth of data and plotting all IV curves, shown in Figure 8. Then, for each IV curve, I extracted $R_{Shunt}$ from it using the technique developed in SPICE. Since $R_{Shunt}$ can be extracted from just one IV curve, I was able to plot its value over the course of a day and look for possible unwanted dependencies on other variables. The result is shown in Figure 9.

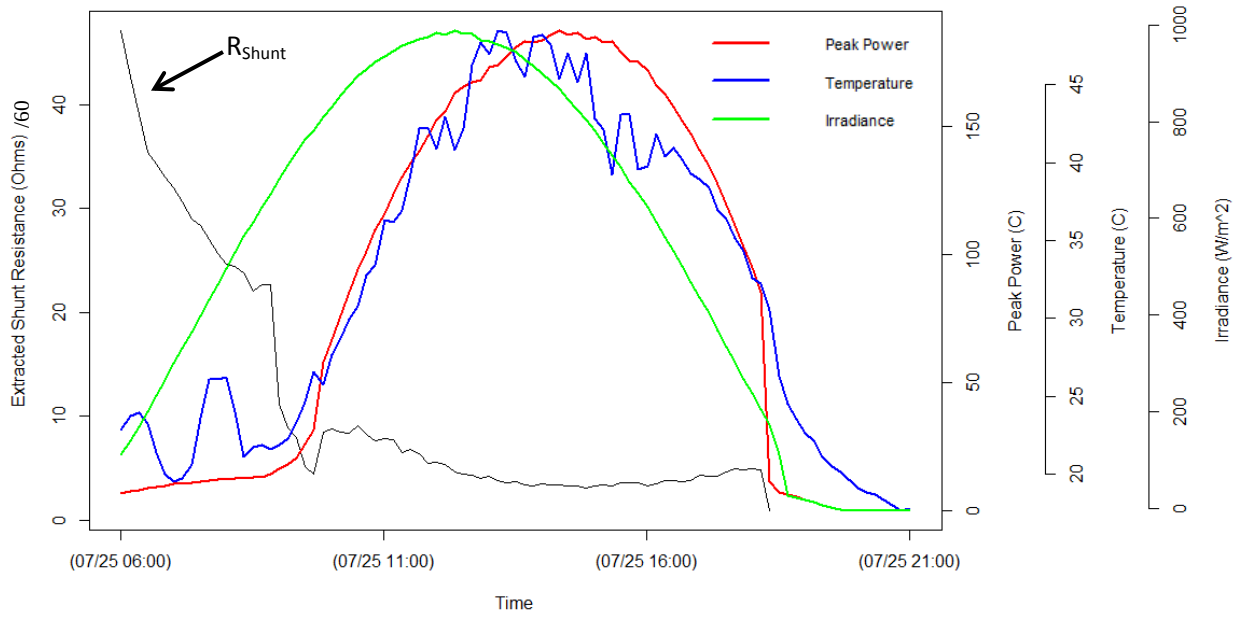


Figure 9: $R_{Shunt}$, Peak power, Temperature, and Irradiance for a single solar panel on July 25, 2013. Note that the tracker wasn't tracking during this day, so the time at which peak power reaches a maximum is when the sun happens to be facing the tracker's position, and not when the sun reached its highest point in the sky. The green line does not represent irradiance incident on the panel, but overall irradiance for a detector facing straight up.

As expected and predicted by literature, the determination of $R_{Shunt}$ becomes highly inaccurate and variable during low irradiance. As irradiance (and thus peak power) increase, the extracted value of $R_{Shunt}$ levels off and has a relatively small variance. These results were promising. By extracting the parameter value during solar noon plus or minus ~2 hours, a good estimate can be obtained.

To determine series resistance, multiple I-V curves are required. So, I used all I-V curves from this day to determine one value of $R_{Series}$. For each I-V curve, I extracted $\left|\frac{dV}{dI}\right|_{I=0}$, $I_{SC}$, $V_{OC}$,

and $R_{Shunt}$. I then plotted $\left|\frac{dV}{dI}\right|_{I=0}$ vs. $\left(I_{SC} - \frac{V_{OC}}{R_{Sh}}\right)^{-1}$. Each point in Figure 10 is obtained from a single I-V curve.

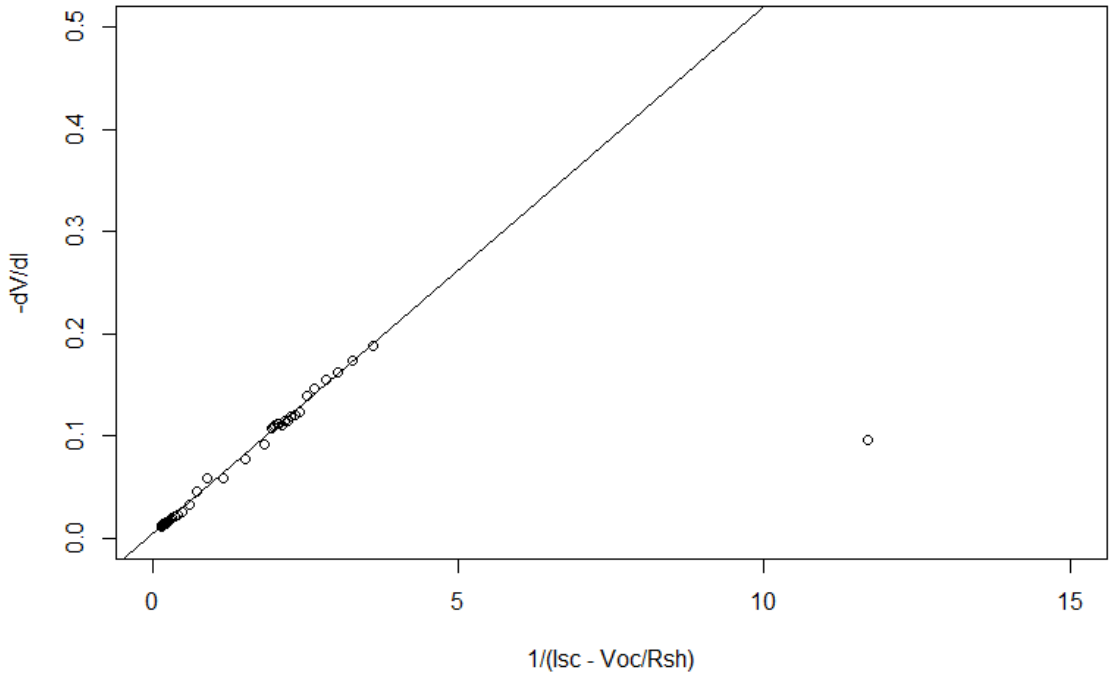


Figure 10: Each data point represents one I-V curve from July 25, 2013. The data fit well on a straight line, indicating that series resistance can safely be approximated as the y-intercept of the straight line fit. Y-axis units are Ohms and x-axis units are $Amps^{-1}$.

With the exception of one outlier, the points appeared to sit on a straight line as expected. I fit a straight line to this data and extracted the y-intercept to be 0.26 Ω. The $R^2$ for the fit was 0.998, an indicator that it was a good fit.

The slope of the best-fit line is equal to $^{nk_BT}/_{q}$, indicating that all I-V curves should have been recorded while the panel is the same temperature. However, because this panel is in the real world, its temperature varies greatly over the course of a day. So, this variation in temperature, ranging from 20 to 45 $^{o}$C, became a source of error for the determination of $R_{Series}$. In order to use the slope of the line to determine the ideality factor *n*, more work must be done to determine how to account for varying temperature. This work would include using

simulations to determine if an average of temperature should be used, and if so how this error propagates through the determination of $R_S$ and *n*.

### 4.3.2 *Whole Year*

After developing these techniques and testing them extensively on both simulated and real data, I hoped to produce plots of parameter values over the course of a year. The goal was to relate the previously established performance metric of fill factor to changes in series or shunt resistance. Fill factor (FF) ranges from 0 to 100% and measures the ratio of its power output to its theoretical maximum power output. It's equal to the product of the current and voltage of its maximum power point ($M_{PP}$) divided by the product of short circuit current and open circuit voltage. As such, it measures the "sagging" of the I-V curve. Clearly, and increasing series resistance or decreasing shunt resistance will act to degrade the FF.

$$FF = \frac{M_{PP}}{I_{SC}V_{OC}} \tag{5}$$

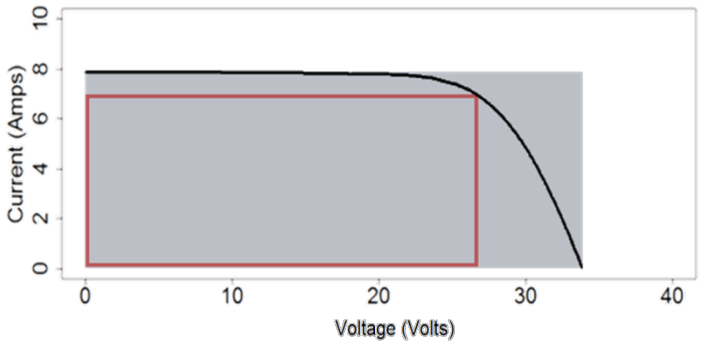


Figure 11: The fill factor is the ratio of the areas of the red box to the grey box. A decreasing fill factor is directly indicative of changing series or shunt resistance (see Figure 8). Degradation resulting in less light reaching the semiconductor is not generally expressed in fill factor, since the entire I-V curve simply shifts downward.

Since the XML files contained FF for each I-V curve, I was able to easily extract it and look at its value for a single panel over the course of a year. I extracted and averaged the FF for one

week, every three months, ranging from March 2013 to March 2014. The measure of FF at lower power output is highly variable and inaccurate, so I began by considering only FF for I-V curves with $M_{PP}$ over 10 Watts. I then applied Chauvenet's criterion to remove outliers as follows. Calculate the mean and standard deviation of the data. For each data point, use the normal distribution function to calculate the probability that the data point will be at its given value. Then, multiply this probability by the number of data points taken. If the resulting value is below 0.5, remove it from the data set. RStudio made it easy to loop through thousands of data points and calculate the Gaussian for each.

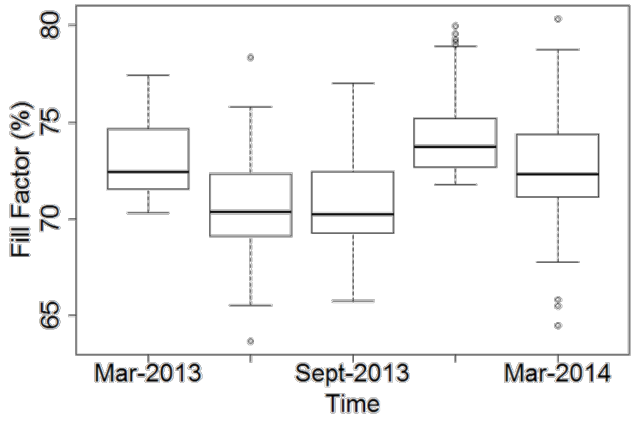


Figure 12: Each box plot represents the average of fill factor over a week for a Canadian Solar 1x module. The solid line represents the median for that week, and 50% of values fall inside the box. The whiskers above and below the boxes represent minimum and maximum values. Single points are outliers not caught by Chauvenet's criterion.

For each of the weeks selected, I generated a bar plot as shown in Figure 12. Clearly, the panel's FF has not yet changed significantly yet. Its change remains within the error bars and so performing extensive parameter extraction on all this data is not worth while at this point in time. Future work will certainly include applying the techniques I have developed to this data once a significant degradation has occurred.

# Conclusion

This project began with the goal of analyzing SunFarm data for insights into degradation via the simulated model. Unfortunately, this objective was not completed due to the lack of observed fill factor degradation. However, most preparation has been completed and the techniques are well understood. This has been achieved through extensive SPICE simulations and verification though analysis of some SunFarm data. The techniques prove to be stable during peak operating hours of each day. The lack of parameter extraction accuracy in low power I-V curves is due to the lack of resolution in the I-V curve tracers at low power and the assumptions and approximations that must be made. In discovering this behavior, I have verified the findings of the literature and extensively verified the techniques developed by Khan et al.

Future work will involve more simulations to further verify and understand the extraction of series resistance in varying irradiance and temperature. This is because no previous literature has explored the error associated with real world I-V curves and instead focuses on laboratory testing. After that, the techniques should be applied to large data sets of I-V curves over time. It would be beneficial for the techniques to be applied to PV panels that are also being analyzed using previously developed L&DS techniques. The findings of the two different analyses could be compared and possibly used together to generate new insight into panel degradation.

# Appendix A: Example R Code

```
#default
par(mar=c(5,4,4,2)+.1)
# for this plot to increase margins for big text
par(mar=c(5, 5, 4, 2) + 0.1)

#===== PACKAGES
 library("chron") # Handles date and time objects

#===== IMPORT NON-IV DATA
 mod209_weekOf_2013_03_25 <- read.csv("209_sa18148-00.csv")

#===== ADD DATETIME OBJECTS TO DATAFRAMES
   dateTime_weekOf_2013_03_25 <- chron(
    dates=sapply(mod209_weekOf_2013_03_25$Date, as.character),
    times=sapply(mod209_weekOf_2013_03_25$Time, as.character))

   #add dateTime_weekOf_2013_03_25 object to original frame
   mod209_weekOf_2013_03_25$dateTime <- dateTime_weekOf_2013_03_25
   #sort by date&time, incase the values weren't entered in the csv properly
   mod209_weekOf_2013_03_25 <-
         mod209_weekOf_2013_03_25[order(mod209_weekOf_2013_03_25$dateTime), ]
   #now we dont need the individual dateTime_weekOf_2013_03_25 object
   remove(dateTime_weekOf_2013_03_25)
 #== END WEEK OF 2013/03/25

#===== AVERAGE TEMP AND IRR
   mod209_weekOf_2013_03_25$Temp_avg <- (mod209_weekOf_2013_03_25$Temp_before
+ mod209_weekOf_2013_03_25$Temp_after)/2
   mod209_weekOf_2013_03_25$Irr_avg <- (mod209_weekOf_2013_03_25$Irr_before +
mod209_weekOf_2013_03_25$Irr_after)/2

#===== FILTER OUT LOW POWER AND CHAUVENET'S CRITERION ON FillFactor

 means <- data.frame(c(1:5), c(1:5))
 colnames(means) <- c("mean", "stdev")

 # DONT CONSIDER FillFactor POINTS WHEN THE POWER IS BELOW THIS VALUE
 minpower <- 10

 entireDateTime <- chron(dates=c("03/25/2013", "04/01/2013"), times=c("00:00:00",
"00:00:00"))
 for(i in seq(1, length(mod209_weekOf_2013_03_25[,1]), 1)) {
  if(mod209_weekOf_2013_03_25$PeakPower[i] < minpower) {
```

```
    mod209_weekOf_2013_03_25$FillFactor[i] <- NA
   }
  }

  # ignore NA values with na.rm = TRUE
  mean <- mean(mod209_weekOf_2013_03_25$FillFactor, na.rm=TRUE)
  sd <- sd(mod209_weekOf_2013_03_25$FillFactor, na.rm=TRUE)

  # APPLY Chauvenet's criterion
  for(i in seq(1, length(mod209_weekOf_2013_03_25[,1]), 1)) {
   if(!is.na(mod209_weekOf_2013_03_25$FillFactor[i])){
    if(((1/(sd*sqrt(2*pi)))*exp(-(mod209_weekOf_2013_03_25$FillFactor[i]-
mean)^2/(2*sd^2)))*length(mod209_weekOf_2013_03_25[,1]) < 0.5) {
      mod209_weekOf_2013_03_25$FillFactor[i] <- NA
    }
   }
  }

  plot(entireDateTime, c(0, 100), type="n", xlab="Date & Time", ylab="Fill Factor")
  abline(h=(seq(0,100,20)), col="lightgray", lty="solid") # add horizontal lines at 0, 20, etc.

  lines(mod209_weekOf_2013_03_25$dateTime,
      mod209_weekOf_2013_03_25$FillFactor, type="p")

  mean <- mean(mod209_weekOf_2013_03_25$FillFactor, na.rm=TRUE)
  sd <- sd(mod209_weekOf_2013_03_25$FillFactor, na.rm=TRUE)

  means$mean[1] <- mean
  means$stdev[1] <- sd

#===== PLOT FF
  entireDateTime <- chron(
   dates=c("03/25/2013", "04/02/2014"),
   times=c("00:00:00", "00:00:00"),
   out.format=c(dates="m-yyyy", times="h:m"))

  plot(entireDateTime, c(0, 100), type="n", xlab="Date & Time", ylab="Fill Factor",
      cex.lab=2, cex.axis=2, cex.main=2, cex.sub=2)
  abline(h=(seq(0,100,20)), col="lightgray", lty="solid")

  lines(mod209_weekOf_2013_03_25$dateTime,
      mod209_weekOf_2013_03_25$FillFactor, type="p")
```

# Appendix B: Design

*Problem statement*

It was unclear from literature exactly how much of the I-V curve to fit a straight line to for the extraction of shunt resistance. Clearly, I could have looked at each I-V curve and fit the line to the part that looked linear. This creates several problems. First, I needed to develop these techniques to be quick and automated so that thousands of I-V curves could be looped through by an R script. Second, it would introduce too much variation in the determination of shunt resistance. I have shown that fitting the straight line to just one extra data point changes the shunt resistance prediction significantly. So, it was necessary for me to design an experiment to determine a standard range of points to fit a straight line to.

The second design aspect to this project was building the circuit in SPICE to run this experiment. It was not obvious how to build the simulated model in a circuit simulator and generate I-V curves from it.

*Constraints*

The techniques I developed needed to be quick, accurate, have a well understood error, and be consistent. The circuits that I built in SPICE needed to be tunable to generate an I-V curve with known parameter values. They also needed to be able to step through many values of a parameter and generate large amounts of I-V curves.

*Approaches*

The obvious approach was to consult the literature. However, the findings of literature concerning parameter extraction techniques are highly variable and subject to their own constraints and apparatus. I chose to answer the question by generating I-V curves in SPICE with known parameter values. This allowed me to analyze the percent error in the extraction techniques. See section 3.3 of this report for the details of the process I designed to answer the question.

As for the design of the circuit, SPICE appeared to be the only answer. Other circuit simulators such as MultiSim are very expensive and more difficult to use. SPICE itself is a command line interface with no built in graphics abilities. The program I used is called LTspice, which is a free SPICE simulator with a GUI that allows the user to click and drag circuit components and see the plots inside of the program.

Each point on an I-V curve represents a static operating point of the circuit. I first tried generating I-V cures in SPICE by attaching a resistor to the circuit and varying its value, recording the voltage and current across it at each step. This wasn't the optimal solution because I wasn't able to get the I-V curve to extend from short circuit current to open circuit voltage. SPICE doesn't allow a resistor to have 0 or infinity Ohms. So, I used a load circuit component with a variable current. Varying the current through the load from 0 to ~10 Amps allowed me to trace out the entire I-V curve. Even though it was traced backwards due to the behavior of the load, and the I-V curve was traced for a little bit of negative voltage, this was the most ideal possible solution.

### *Analysis*

See section 3.4 of this report for details on the analysis of these methods. The approach that I designed to answer the question seemed like the only logical one. By trying to fit a straight line to every subset of the I-V curve containing the left-most data points, I was certain to find the best solution.

### *Iterations*

I repeated the approach several times and generated many plots like the one in Figure 7. I also varied the noise that was added to the I-V curve to analyze the dependence of the techniques on noise. However, this was purely exploratory because the I-V curve tracer documentation listed the percent noise in its measurements. Since the methods that I designed answered my question right away, there were no iterations on the process itself.

# References


[1] L. S. Bruckman, N. R. Wheeler, J. Ma, E. Wang, C. K. Wang, I. Chou, J. Sun, and R. H. French, "Statistical and Domain Analytics Applied to PV Module Lifetime and Degradation Science," *IEEE Access*, vol. 1, pp. 384–403, 2013.

[2] R. H. French, M. P. Murray, W.-C. Lin, K. A. Shell, S. A. Brown, M. A. Schuetz, and R. J. Davis, "Solar radiation durability of materials components and systems for Low Concentration Photovoltaic Systems," in *2011 IEEE Energytech*, 2011, pp. 1 –5.

[3] Y. A. Mahmoud, W. Xiao, and H. H. Zeineldin, "A Parameterization Approach for Enhancing PV Model Accuracy," *IEEE Trans. Ind. Electron.*, vol. 60, no. 12, pp. 5708–5716, Dec. 2013.

[4] J. L. Gray, "The physics of the solar cell," *Handb. Photovolt. Sci. Eng.*, p. 12, 2003.

[5] F. Khan, S. N. Singh, and M. Husain, "Effect of illumination intensity on cell parameters of a silicon solar cell," *Sol. Energy Mater. Sol. Cells*, vol. 94, no. 9, pp. 1473–1476, Sep. 2010.

[6] D. Sera and R. Teodorescu, "Robust series resistance estimation for diagnostics of photovoltaic modules," in *35th Annual Conference of IEEE Industrial Electronics, 2009. IECON '09*, 2009, pp. 800–805.

[7] M. Wolf and H. Rauschenbach, "Series resistance effects on solar cell measurements," 1963.

[8] Priyanka, M. Lal, and S. N. Singh, "A new method of determination of series and shunt resistances of silicon solar cells," *Sol. Energy Mater. Sol. Cells*, vol. 91, no. 2–3, pp. 137–142, Jan. 2007.

[9] T. J. McMahon, T. S. Basso, and S. R. Rummel, "Cell shunt resistance and photovoltaic module performance," in *, Conference Record of the Twenty Fifth IEEE Photovoltaic Specialists Conference, 1996*, 1996, pp. 1291–1294.

[10] A. D. Dhass, E. Natarajan, and L. Ponnusamy, "Influence of shunt resistance on the performance of solar photovoltaic cell," in *2012 International Conference on Emerging Trends in Electrical Engineering and Energy Management (ICETEEEM)*, 2012, pp. 382–386.

[11] K. Ishaque, Z. Salam, H. Taheri, and Syafaruddin, "Modeling and simulation of photovoltaic (PV) system during partial shading based on a two-diode model," *Simul. Model. Pract. Theory*, vol. 19, no. 7, pp. 1613–1626, Aug. 2011.

[12] M. Bashahu and P. Nkundabakura, "Review and tests of methods for the determination of the solar cell junction ideality factors," *Sol. Energy*, vol. 81, no. 7, pp. 856–863, Jul. 2007.

[13] D. Pysch, A. Mette, and S. W. Glunz, "A review and comparison of different methods to determine the series resistance of solar cells," *Sol. Energy Mater. Sol. Cells*, vol. 91, no. 18, pp. 1698–1706, Nov. 2007.

[14] E. Cuce, P. M. Cuce, and T. Bali, "An experimental analysis of illumination intensity and temperature dependency of photovoltaic cell parameters," *Appl. Energy*, vol. 111, pp. 374–382, Nov. 2013.

[15] K. Ishibashi, Y. Kimura, and M. Niwano, "An extensively valid and stable method for derivation of all parameters of a solar cell from a single current-voltage characteristic," *J. Appl. Phys.*, vol. 103, no. 9, pp. 094507–094507–6, 2008.

[16]F. GHANI, M. Duke, and J. Carson, “Extraction of solar cell modelling parameters using the Lambert W function,” in *Proceeding of the annual conference, Australian solar energy society, Melbourne*, 2012.
[17]F. Ghani and M. Duke, “Numerical determination of parasitic resistances of a solar cell using the Lambert W-function,” *Sol. Energy*, vol. 85, no. 9, pp. 2386–2394, 2011.
[18]F. Ghani, M. Duke, and J. Carson, “Numerical calculation of series and shunt resistance of a photovoltaic cell using the Lambert W function: Experimental evaluation,” *Sol. Energy*, vol. 87, pp. 246–253, 2013.
[19]Z. Salam, K. Ishaque, and H. Taheri, “An improved two-diode photovoltaic (PV) model for PV system,” in *2010 Joint International Conference on Power Electronics, Drives and Energy Systems (PEDES) 2010 Power India*, 2010, pp. 1–5.
[20]D. Sera, “Series resistance monitoring for photovoltaic modules in the vicinity of MPP,” in *25th European Photovoltaic Solar Energy Conference and Exhibition*, 2010, pp. 4506–4510.
[21]C. D. Ferris, “Spice for Electronics.” West Publishing Company, 1995.